PHYSICS OF MRF REGULARIZATION FOR SEGMENTATION OF MATERIALS MICROSTRUCTURE IMAGES

Jeff Simmons,[†] Craig Przybyla,[†], Stephen Bricker,[*]Dae Woo Kim,[‡] Mary Comer[‡]

[†]Materials and Manufacturing Directorate, Air Force Research Laboratory, Dayton, OH 34433
[*]Department of Electrical and Computer Engineering, University of Dayton, Dayton, OH 45469
[‡]Department of Electrical and Computer Engineering, Purdue University, West Lafayette, IN 47907

ABSTRACT

The Markov Random Field (MRF) has been used extensively in Image Processing as a means of smoothing interfaces between differing regions in an image. The MRF applies a total boundary length 'energy' penalty that is subsequently minimized by an inversion algorithm. Minimum energy implies a force associated with boundaries, the sum of which must equal zero at every point at equilibrium. This requirement leads to long range structures, resulting from the short-range interactions of the MRF used to bias segmentation results. This work uses a simple Bayesian MRF regularized segmentation method to show that classical results from Surface Science are reproduced when segmenting regions of low contrast. This has implications, both in the Materials Science and Image Processing fields.

Index Terms— segmentation, priors, context-sensitive segmentation, materials science

1. INTRODUCTION

In Materials Science, properties of materials are modified by changing the 3-D texture ('microstructure,' in the Materials literature). Much attention has been historically directed towards characterizing this microstructure via various modalities of microscopy. Script-driven image collection makes it possible to collect large datasets over night, from which more complete characterizations can be made. Consequently, attention has been directed towards automating the analysis of the image data. To this end, we have begun to work with regularized methods, typically using the Markov Random Field (MRF)[1] and the Generalized Gaussian Markov Random Field (GGMRF).[2, 3, 4]

MRF regularization is based on the Ising model, which was originally developed to describe physical systems. This introduces a double edged sword of providing 'good' segmentations of an image, while introducing a bias that can produce physically justifiable erroneous results. This paper introduces the concepts of Surface Science, which are implicit in the Ising model, and can produce unexpected results. Several of the classical results from Surface Science

are shown that are reproduced in MRF regularized segmentations.

The parallel development of the MRF in Solid State Physics, Materials Science, and Image Processing are described in the Prior Work section. The segmentation method, introductory Surface Science, and specific segmentation methods are discussed in the Methods section. The Results, Discussion, and Conclusion sections follow suite. We discuss the implications of Surface Science in both Materials Science and Image Processing fields in the Discussion.

2. PRIOR WORK

The Ising Model was developed in Physics by Ernst Ising[5, 6] as a means of analyzing the phase transition behavior of a 1-D ferromagnet. This was extended to a 2-D ferromagnet by Onsager.[7] By hypothesis, at equilibrium, the probabilities of states of points in Ising lattices are Gibbs distributed (Boltzmann distributed in the Physics literature). The Ising model has only two possible spin states, a limitation that was lifted with the Potts model,[8, 9] which allowed multiple states. Binder, developed Monte Carlo methods for computation of thermodynamic properties of these systems, using Metropolis importance sampling.[10]

In parallel, MRFs have become ubiquitous in the image processing and computer vision literature. The Hammersley-Clifford theorem[11] showed that a random field is an MRF if and only if it has a Gibbs distribution. This allows an MRF to be constructed using localized conditional probabilities, with a joint distribution that can be written in terms of an energy function. This theorem was never published, but Besag[12] published a proof. Geman and Geman[13] proposed a Markov chain Monte Carlo sampling approach (Gibbs sampler), that allows determination of the maximum a posteriori (MAP) estimate of an image. Marroquin, *et al.*,[14] proposed a method based on the Gibbs sampler for approximating the maximum of the posterior marginals (MPM) estimator.

In the Materials literature, the Ising and Potts models were developed into evolution models that described *mesoscale structures*, i.e. collective patterns of aggregates of

pixels on a scale intermediate between the pixel and continuum scales. Principal developers of these techniques included Liebowitz, *et al.*[15] and Srolovitz, *et al.*,[16][17] although the technique has been used extensively by many authors. Miodownik, *et al.*[18] used Monte Carlo methods to validate a mechanism proposed by Zener (Zener pinning) by which interfaces become trapped by small particles. The reviews by Landau and Binder[19] and by Rollett and Manohar[20] summarize key developments.

To the best of the authors' knowledge, this is the first time mesoscale structure implications of the MRF and their influence on MRF-regularized segmentation have been investigated.

3. METHODS

Mesoscale structures originate from the collective behaviors of local interactions in solids and have also been shown to develop in simulations involving Potts models.[15, 16] The MRF, being one of the most common forms of smoothing and having been derived from these models, is expected to bias the results of a segmentation to produce mesoscale structures. This section describes the MRF regularized segmentation method used here and gives a brief description of mesoscale structures predicted by Surface Science.

3.1. Regularized Segmentation

The EM/MPM algorithm[21] is a Bayesian method that uses a mixture of Gaussians to model the observed image and an MRF for regularization and uses minimization of the expected number of misclassified pixels as an estimation criterion. Built on the MPM[14] model, it uses an EM algorithm to estimate the parameters in the image model. It has been applied to Materials Science images in previous work.[1] The codes we used here are available online as the EM/MPM Workbench at www.bluequartz.net.

Let $\mathbf{X}$ and $\mathbf{Y}$ be the segmentation label field (to be estimated) and the observed image, respectively. Both are defined on rectangular lattice, S, such that the random variables $X_s \in \mathbf{X}$ and $Y_s \in \mathbf{Y}$ occur at the spatial location $s \in S$.

In this paper, $\mathbf{x} \triangleq (x_1, x_2, \cdots, x_N)$ represents a sample realization of $\mathbf{X} \triangleq (X_1, X_2, \cdots, X_N)$ and, similarly for $\mathbf{y} \triangleq (y_1, y_2, \cdots, y_N)$, where N is the number of points in S. The MRF model used here is a K-level Ising model: $x_s \in \{1, 2, 3, \ldots, K\}$, where K is the number of possible classes, with probability mass function of $\mathbf{X}$ modeled as:

$$p_{\mathbf{X}}(\mathbf{x}) = \frac{1}{z} \exp\left(-\sum_{\{r,s\}\in\mathscr{C}} \beta_{x_r,x_s}(1-\delta_{x_r,x_s})\right) \qquad (1)$$

where $\mathscr{C}$ is a collection of cliques, β_{x_r,x_s} are spatial interaction parameters (dimensionless exchange energies in the Physics literature), and δ_{x_r,x_s} is Kroneker's delta function of x_r and x_s.

The observation is modeled according to:

$$f_{\mathbf{Y}|\mathbf{X}}(\mathbf{y}|\mathbf{x},\boldsymbol{\theta}) = \prod_{r=1}^{N} \frac{1}{\sqrt{2\pi\sigma_{x_r}^2}} \exp\left(-\frac{(y_r-\mu_{x_r})^2}{2\sigma_{x_r}^2}\right) \qquad (2)$$

where θ is the set of parameters to be estimated for the Gaussians: mean (μ_k) and variance (σ_k^2) for every class k.

Using Equations (1) and (2), Bayes' rule gives:

$$p_{\mathbf{X}|\mathbf{Y}}(\mathbf{x}|\mathbf{y},\boldsymbol{\theta})$$

$$= \frac{1}{z f_{\mathbf{Y}}(\mathbf{y}|\boldsymbol{\theta})} \left[\prod_{r=1}^{N} \frac{1}{\sqrt{2\pi\sigma_{x_r}^2}}\right]$$

$$\exp\left(-\sum_{r=1}^{N} \frac{(y_r-\mu_{x_r})^2}{2\sigma_{x_r}^2} - \sum_{\{r,s\}\in\mathscr{C}} \beta_{x_r,x_s}(1-\delta_{x_r,x_s})\right) \qquad (3)$$

where z is the partition function and $f_{\mathbf{Y}}(\mathbf{y}|\theta)$ is the marginal probability of y for parameters θ.

The EM/MPM algorithm is implemented by alternately executing the MPM algorithm for segmentation and the EM algorithm for the parameter estimation until some stopping criterion has been met.

3.2. Surface Science

Thermodynamics includes the study of properties of homogeneous volumes of materials, or *phases*, as well as the boundaries between them. The later subject is a well developed field: *Surface Science* (for recent reviews, see[22, 23, 24]). The classical topic of Surface Science was developed by Gibbs[25] and contemporaries and involves the interplay between interfaces with other interfaces, as well as phases. When a length penalty is used on an interface, all of these factors come into play.

One key result can be seen by considering a 2-D image containing a junction of interfaces that can migrate in order to establish equilibrium. If the junction is located at a point (x, y), by hypothesis, the energy ($E(x, y)$) is single valued with an equilibrium state described by:

$$E^{eq} = \{E^{eq} | E(x, y) - E^{eq} \geq 0, \ \forall (x, y) \in R^2\} \qquad (4)$$

Far from a critical point, $E(x, y)$ may be expanded in a Taylor's series about E^{eq}:

$$E = E^{eq} + \sum_{i=1}^{3} \partial E/\partial s_i \Delta s_i + O(||\Delta r||_2^2) \qquad (5)$$

where s_1 are variables that parameterize the intersecting curves and $\Delta r \triangleq (x - x^{eq}, y - y^{eq})$, is a deviation from the equilibrium position.

Changing the partials in Equation (5) to directional derivatives, $\partial/\partial s_i \triangleq \hat{\mathbf{t}} \cdot \nabla$, where $\hat{\mathbf{t}}_i \triangleq \frac{d}{ds_i} R_i(x(s_i), y(s_i))$ are the tangent vectors to the curves. Recognizing that Δs_i is

just $\hat{\mathbf{t}}_i \cdot \Delta r$, and retaining only the principal linear parts of the increments (δE and δr), Equation (5) becomes:

$$\delta E = \delta r \cdot \left(\sum_{i=1}^{3} \hat{\mathbf{t}}_i \hat{\mathbf{t}}_i \cdot \nabla E \right) = 0 \qquad (6)$$

Defining $\hat{\mathbf{t}}_i \cdot \nabla E \triangleq \Gamma_i$ as *interface tensions* that are implicitly defined by the regularization parameters β_{ij}, we can see that they are forces, being derivatives of energies. Substituting into Equation (6), and recognizing that δr being arbitrary requires the sum vanish identically, the sum becomes:

$$\sum_{i=1}^{3} \hat{\mathbf{t}}_i \Gamma_i = 0 \qquad (7)$$

Equation (7) is a classical relationship that *must* be obeyed by all interface junctions in 2-D at equilibrium. One interesting case is *wetting*, where $\Gamma_1 > \Gamma_2 + \Gamma_3$. In this case, boundary 1 is unstable and will be consumed by the others.

The interplay between interfaces and phases is illustrated by the classical capillarity phenomenon. Consider a "tube" in 2-D, as shown in Figure 1(a). If this were filled with a fluid, equilibrium would obtain when the "volume force" due to gravity on the fluid in the cavity equaled the jump in interface tensions at the junction of the fluid interface with the walls of the tube:

$$\iint \rho g \, dh \, dr = 2[\![\Gamma]\!] \qquad (8)$$

where ρ is the "density" of the fluid, g is a "gravitational force," h is the hight above "equilibrium surface height" of a reservoir, $2r$ is the thickness of the tube, and $[\![\Gamma]\!]$ is the jump in interface tensions at the junction. In an image analogy, ρg would describe the mismatch of forward models and $[\![\Gamma]\!]$ is implicitly defined by the mismatch in β hyperparameters.

Finally, interfaces can combine by intersection with others, leading to "binding energy" of an interface to a small region, if some length of interface can be consumed with the intersection. Zener[26] pointed this out and proposed a mechanism by which boundaries of crystallites can be "pinned" by small particles because, when a boundary intersects a particle, the total boundary area is reduced by the cross sectional area of the particle. This is commonly referred to as *Zener pinning*.

3.3. Regularized Segmentation with Low Contrast

Regularized segmentation is a balance between the observation and the regularization. In the extreme where there is very little intensity difference between regions, the regularization dominates. This work exploits an artifact in the forward model: being a mixture of Gaussians, a shallow gradient will segment as two regions, each region being defined by its respective Gaussian. Since there is almost no contrast in the original image, the (hallucinated) boundary

between these regions should show the mesoscale behavior dictated by Surface Science. Inputs were prepared, either as phantoms with gentle gradients and some Poisson noise added to simulate detector noise, or from real images of a Silicon Carbide fiber/matrix composite, where the fibers had a coating material. The background (matrix) in those images often have small gradients in intensity due to imaging irregularities. These were cropped and used for inputs.

Four phenomena were investigated: capillarity elevation, contact angles, wetting, and Zener pinning, as described above. Only qualitative features were sought because of the difficulties of evaluating Γ values from β values (discussed below). In all cases, at least 5 segmentations were performed under the same conditions and the results reported were typical of the set.

4. RESULTS

Figure 1(a) shows the phantom used for to show capillarity effects. The darker outside regions segment as the same class and the central portion (the 'tube') is designed to segment as two classes. Figure 1(c) shows an 'unbiased' segmentation for which β for all interfaces are equal to 0.9. The low contrast boundary is half way up the tube.

Choosing a larger value (2.0) for β for the lower portion of the tube wall and a smaller value (1.4) for the upper portion produced the predicted result: depression of the meniscus, as shown in Figure 1(b). Reversing the β values had the opposite effect (Figure 1(d)).

None of the segmentations reliably reproduced Equation (7), presumably because of the ill-defined values of Γ for small systems (discussed below).

Figure 2(a) shows a SiC/SiC composite with a slight gradient in the intensity of the background (inset). Figure 2(b) shows a three class segmentation of the inset, where classes 0, 1, and 2 are the red, light gray, and dark gray regions, respectively. Increasing $\beta_{1,2}$ favors interfaces with class 0, which completely wetted the interface, See Figure 2(c).

Figure 3 shows a segmentation of the same sample with
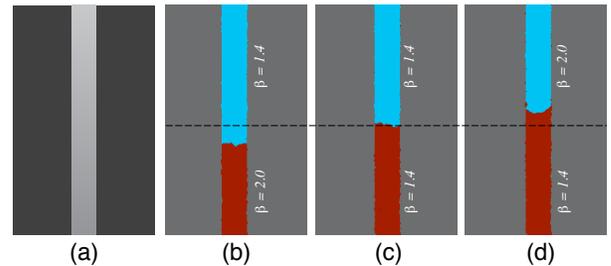
Fig. 1. Capillarity induced segmentations observed when a gentle gradient exists in intensity of the center region. (a) phantom, (b-d) effects of boundary penalty differences.
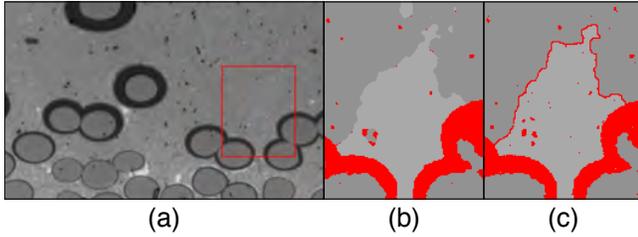
Fig. 2. Regularization induced wetting of an interface. (a) original image, (b) $\beta_{0,1} = 0.9$, $\beta_{0,2} = 0.5$, $\beta_{1,2} = 0.9$, (c) $\beta_{0,1} = 0.9$, $\beta_{0,2} = 0.9$ and $\beta_{1,2} = 1.8$.

a low contrast boundary. The circled areas indicate inclusion particles that segment as a dark gray class, which, apparently, pin the boundaries as Zener predicted.

5. DISCUSSION

The results of the segmentation show qualitative agreement with the predictions of Surface Science. It is likely that true quantitative agreement will not be possible for several reasons. Most importantly, Surface Science is an asymptotic theory, which applies in the limit as the discretization scale tends to zero. For the results shown here, the pixel size was significant in comparison with the feature size. In this case, $\{\Gamma_i\}$ are stochastic properties that are parameterized by $\{\beta_i\}$, fluctuating from one segmentation to another. Possibly, $\{\Gamma_i\}$ can be estimated, as has been done by Mon, *et al.*,[27] but this requires identification of a characteristic energy and a temperature to be defined.

The implications of mesoscale behavior of boundaries affects image processing in Materials Science directly because materials behavior is typically dominated by multiple length scales. For example, fracture behavior is often determined by the properties of the interfaces between phases, which is dominated by the atomic scale, typically $0.1nm$. On the other hand, strength is often determined by textures, whose characteristic length scale is typically 0.5μ or larger. In evolution simulations, segmented structures form

Fig. 3. Segmentation showing the Zener pinning mechanism with a low contrast boundary.

boundary conditions for Partial Differential Equation (PDE) based simulations, so interface detail is critically important.

Analysis of mesoscale behavior is important in image segmentation because it explains some of the global effects of MRF regularization, particularly when the results of a segmentation do not match expectations, e.g. Figure 3. For inpainting,[28] if the boundary between two inpainted regions is important, the values of $\{\beta\}$ can be used to control the characteristics of extrapolations. The wetting behavior presented above shows promise for cases where it is desired to keep objects from aggregating in segmentations, though further development is needed to separate same-class objects.

6. CONCLUSIONS

It was shown that longer range 'mesoscale' structure development can occur with MRF regularized segmentations that mirror known phenomena in Surface Science. It was argued that these effects can be exploited for inpainting, with applications in both Materials Science and Image Processing.

7. ACKNOWLEDGEMENTS

8. REFERENCES

[1] M. Comer J.E. Spowart M.D. Uchic M. De Graef J.P. Simmons, P. Chuang, "Application and further development of advanced image processing algorithms for automated analysis of serial section image data," *Modelling and Simulation in Materials Science and Engineering*, vol. 17, pp. 025002, 2009.

[2] Michael Jackson Marc De Graef Jeff Simmons Charles A. Bouman Singanallur V. Venkatakrishnan, Lawrence F. Drummy, "A model based iteratirve reconstruction algorithm for high angle annular dark field - scanning transmission electron microscope (haadf-stem) tomography," *IEEE Transactions on Image Processing*, vol. 22, pp. 4532–4544, 2013.

[3] Michael Jackson Marc De Graef Jeff Simmons Singanallur Venkatakrishnan, Lawrence Drummy and

Charles Bouman, "Bayesian tomographic reconstruction for high angle annular dark field (haadf) scanning transmission electron microscopy (stem)," in *Statistical Signal Processing Workshop (SSP)*. IEEE, 2012, pp. 680–683.

[4] Jeff P. Simmons Charles A. Bouman Singanallur V. Venkatakrishnan, Lawrence F. Drummy Marc De Graef, "Model based iterative reconstruction for bright field electron microscopy," in *IS&T/SPIE Electronic Imaging*. International Society for Optics and Photonics, 2013, pp. 86570A–86570A.

[5] E. Ising, *Beitrag zur Theorie des Ferro- und Paramagnetismus*, Ph.D. thesis, University of Hamburg, 1924.

[6] E. Ising, "A contribution to the theory of ferromagnetism," *Z. Phys*, vol. 31, pp. 253–258, 1925.

[7] Lars Onsager, "Crystal statistics. i. a two-dimensional model with an order-disorder transition," *Phys. Rev.*, vol. 65, pp. 117–149, 1944.

[8] R.B. Potts, *The mathematical investigation of some cooperative phenomena*, Ph.D. thesis, Thesis, Oxford University, 1951.

[9] R.B. Potts, "Some generalized order-disorder transformations," *Proceedings of the Cambridge Philosophical Society*, vol. 48, pp. 106–109, 1952.

[10] K. Binder and H. Rauch, "Calculation of spin-correlation functions in a ferromagnet with a monte carlo method," *Physics Letters A*, vol. 27, pp. 247–248, 1968.

[11] J. Hammersley and P. Clifford, "Markov fields on finite graphs and lattices," unpublished research, 1971.

[12] J. Besag, "Spatial interaction and the statistical analysis of lattice systems," *Journal of the Royal Statistical Society B*, vol. 36, pp. 192–236, 1974.

[13] S. Geman and D. Geman, "Stochastic relaxation, gibbs distributions, and bayesian restoration of images," *IEEE Journal on Pattern Analysis and Machine Intelligence*, vol. 6, pp. 721–741, 1984.

[14] S. Mitter J. Marroquin and T. Poggio, "Probabilistic solution of ill-posed problems in computational vision," *Journal of the American Statistical Association*, vol. 82, pp. 76–89, 1987.

[15] J.L. Lebowitz A.B. Borz, M.H. Kalos, "A new algorithm for monte carlo simulation of ising spin systems," *Journal of Computational Physics*, vol. 17, pp. 10–18, 1976.

[16] G.S. Grest P. S. Sahni M.P. Anderson, D.J. Srolovitz, "Computer simulation of grain growth–i. kinetics," *Acta. Metall.*, vol. 35, pp. 783–791, 1984.

[17] David J. Srolovitz Gary Grest, Michael P. Anderson, "Domain-growth kinetics for the q-state potts model in two and three dimensions," *Phys. Rev. B.*, vol. 38, pp. 4752–4760, 1988.

[18] G.N. Hassold M. Miodownik, E.A. Holm, "Highly parallel computer simulations of particle pinning: Zener vindicated," *Scripta Metall.*, vol. 42, pp. 1173–1177, 2000.

[19] David P. Landau and Kurt Binder, *A Guide to Monte Carlo Simulations in Statistical Physics*, Cambridge University Press, New York, NY, 2003.

[20] A.D. Rollett and P. Manohar, "Monte carlo modeling of grain growth and recrystallization," *Continuum Scale Simulation of Engineering Materials*, p. 855, 2004.

[21] Mary L. Comer and Edward J. Delp, "The em/mpm algorithm for segmentation of textured images: Analysis and further experimental results," *IEEE Trans. Image Processing*, vol. 9, pp. 1731–1744, 2000.

[22] David Quéré, "Wetting and roughness," *Annu. Rev. Mater. Res*, vol. 38, pp. 71–99, 2008.

[23] A.I. Rusanov, "Surface thermodynamics revisited," *Surface Science Reports*, vol. 58, pp. 111–239, 2005.

[24] Paul Wynblatt Wayne D. Kaplan, Domique Chatain and W. Craig Carter, "A review of wetting vs. adsorption, complexions, and related phenomena: The rosetta stone of wetting," *J. Mater. Sci*, vol. 48, pp. 5681–5717, 2013.

[25] J.W. Gibbs, "On the equilibrium of heterogeneous substances," *American Journal of Science*, vol. 96, pp. 441–458, 1878.

[26] C.S. Smith, "Equilibrium of iron-carbon-silicon and iron-carbon-manganese alloys with mixtures of methane and hydrogen at 1000°," *Trans. AIME*, vol. 175, pp. 15–51, 1948, cited private communication from C. Zener.

[27] D.P. Landau K. Binder K.K. Mon, S. Vansleben, "Anisotropic surface tension, step free energy, and interfacial roughening in the three-dimensional ising model," *Phys. Rev. Lett.*, vol. 60, pp. 708–711, 1988.

[28] Christine Guillemot and Oliver Le Meur, "Image inpainting," *Signal Processing Magazine*, vol. 31, pp. 127–144, 2014.